An Analytical Method of Recognizing Pulsars at Moderate SNR

Peter East

Preamble: Statistics and Analytics

To recognize a pulsar with confidence after folding, using statistics alone, it is generally agreed that signal-to-noise (SNR) ratios upwards of 6:1 (6 sigma) may be necessary. The level that professionals choose is above 10:1, but of course this is in search mode where mostly, no information on the pulsar presence or parameters is known.

But if collateral information is available, such as,

1. Knowledge of the pulsar parameters, mean flux density, pulse width, pulse repetition interval, scintillation and dispersion, for example.
2. A receiving system that has sufficient calibrated sensitivity to capture the pulsar data and its antenna is pointed in the correct direction for sufficient time.
3. Ability to process the received data to exploit the known parameters to derive pulsar-specific measures[1].
4. An understanding of how these processes react to random noise and RF interference (RFI).

Then by analyzing and predicting the response of period search, p-dot search and dispersion search processes on pulsar data, it is possible to highlight pulsar specific features at much lower SNR levels.

Brought up accepting the limitations of software and digital thresholding, we tend to ignore our brains' ability to recognize patterns. Consider early analog radar operators; with experience of transmitter and target characteristics, they were able to consistently detect targets at tangential signal sensitivity (TSS) on an A-scan cathode-ray tube (CRT) display. TSS is equivalent to 2.5 sigma - their life could depend on it. Indeed, some operators became so skilled that minimum detection sensitivity (MDS) was defined as 3dB or 1.4 sigma[2]. Incidentally, the CRT fast-rise, long-decay phosphors used in A-scan CRT displays actually predate the integration process observed with the folding algorithm. Modern radar digital detection systems[3] require signal-to-noise ratios of 6 to 10 sigma (15dB to 20dB) for reliable indication of random targets, and even more in cluttered environments.

It needs to be understood that once a noise has been recorded and detected the integrated resultant is no longer random. It is determinate, since it is the resultant of a number of recorded random component parts. Large peaks and troughs in the integrated output do not result from a regular or periodic sub-components, but arise from chance dominating features at random points along the record. These also respond in a predictable but different way to pulsars in the search processes. A consistent sub-component may also arise from RFI, however these can usually be identified during search tests.

Introduction

Pulsar recognition and validation after fold processing by large radio telescopes, is conventionally based on identifying a significant pulse or regular pulse train, then carrying out a period search around the known pulsar period to produce a peak at the expected value. This identification can be ratified by performing a dispersion search around the expected pulsar dispersion measure (DM) to similarly produce a peak at the known value. The PRESTO[4] software, used by professionals and high-end amateurs, carries out a similar process automatically. Whilst this works well for processed SNR's greater than 10:1, the period-search and dispersion-search peaks can

be diluted by noise and RFI and also by low duty-cycle pulsar types. For reasons of speed, PRESTO uses the reduced chi-squared test for detection, which reacts well to data distortion from Gaussian noise. It doesn't actually lock to the pulsar peak amplitude, but detects deviations from Gaussian noise from the distorting effect of a large pulse power. This statistical pulsar recognition process can be augmented by the analytical approach described here. This latter approach extends the work of reference (5), providing a mathematical basis for evaluating the period and period rate search characteristics of a finite pulse width semi-continuous pulse train, permitting measures enabling noise and RFI discrimination. Period search and period rate search are to some extent correlated but by careful choice of search parameters, it is possible to track the pulsar pulse train presence along the data record. Applied to dispersion search the analysis permits greater confidence in pulsar identification. Using these techniques, recognition confidence can be extended to much lower signal-to-noise ratios.

Statistical Pulsar Recognition

After applying the folding algorithm, matched to the pulsar period, to detected data records, the resulting output comprises an integrated pulsar pulse sitting on random noise. The noise base consists of the integrated sum of system noise sections of each consecutive period. From statistics central limit theory, the sum of many random noise records tends to a Gaussian/Normal amplitude distribution. This simplifies analysis for, using published tables we know that noise peaks of 3 times the standard deviation (or rms, root-mean-square if the noise data is zero mean) level are expected to occur and be confused with a 3 sigma SNR pulsar pulse with a probability of 1 in a thousand. Whereas noise peaks of 6 sigma are only likely with a probability of 1 in a billion making a pulsar detection at this level a near certainty. Because of the poorer odds below 6 sigma it is recognized that in this region, statistics alone is not a reliable indicator of pulsar presence in the data. RFI is also averaged by the folding process and, if not removed, increases the noise base further lowering the measured SNR. Noise spike RFI are easily eliminated by data limiting but RFI modulations with strong regular components matching the pulsar search frequency can be a problem. Whilst a large pulse and peak period search on their own do not guarantee pulsar detection, the analytical methods described below will confirm the expected pulsar train properties .

Pulsar Period Search Characteristics

Pulsar period search is used to indicate an accurate value for the observed pulsar period by determining the point of pulse amplitude maximum. The data is folded at a number of discrete periods, the period being changed typically in fractional parts per million. Figure 1 depicts the effect of changing the period by *-p* parts per million.

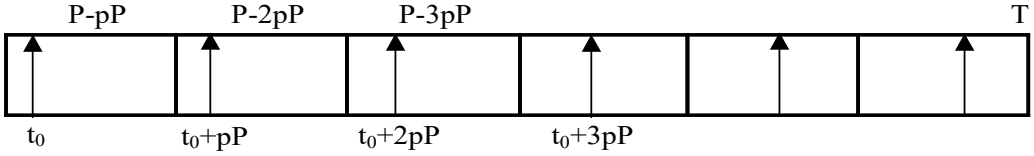

Figure 1. Period Search Parameters

Normally, the total record, covering an observation time *T* is divided into sections equal to the pulsar period *P.* The first pulse arrives at time t_0 after the record start. In the matched period case, the pulsar pulse will occur in the same relative position t_0

and when the sections are summed (or folded), the pulses add linearly and any noise present adds as the detected voltage square root, improving the SNR by the square-root of the number of sections. When the period is reduced by *p* parts per million the pulsar pulse is delayed in increments of *pP* in successive periods as shown in Figure 1. These delays although small will tend to spread the observed pulse and reduce the summed amplitude. Similarly for increasing *p* producing a bell-shaped amplitude profile. The peaking effect is shown in PRESTO, but since we know the pulse width, with this analysis, the amplitude curve shape can be predicted with some accuracy. In addition, it is realized that for pulse train existing over the whole record, given a value of *p*, the apparent stretched pulse width and new pulse center position can also be predicted. This additional predicted information for a continuous pulse train can be compared to actual results to add confidence in real pulsar presence.

In summary, referring to Figure 1, for pulses,

1. When the folding period matches the pulsar period the pulsar pulses align in each fold window and add to maximize pulsar visibility.
2. Decreasing the fold period slightly causes the pulse to increasingly shift later within the fold period window smearing out the pulse.
3. The maximum shift occurs within the last fold period and totals, *NpP* where *pP* is the fold period shift and *N* is the total number of folds.
4. If *T*' is the total observation time, then *N* = *T/P* and the pulse total spread extent is *pT*, where, *p* is the search period change and is normally described in parts per million (ppm).
5. So with *p* ppm search period change the mean pulse width increases by *pT*' and the pulse center position changes to, $t_0 + pT/2$
6. Since the total integrated pulse power is constant, the resulting amplitude/period curve drops to one half, when the observed pulse width, *W* doubles, or, $pT/W = 2$ (see Figure 2.). So now we have a direct measure that confirms a pulsed signal is present for the record duration.
7. In practice the pulse extent and shape and amplitude change are dependant on the pulse scintillation amplitude along the record, and at low signal-to-noise ratios it is also influenced by the underlying noise profile. Further variation occurs if reception is in drift-scan mode due to the receive antenna beam profile. To a first order however, this simple analysis describes the key properties observed in practice.

Assuming the pulsar pulse is similar to a Gaussian shaped pulse of equal half-height width *W*, the fold algorithm can be expressed as,

$$Fold(t) = \frac{1}{N}\sum_{n=1}^{N} A(n)\exp\left(-4\ln(2)\left[\frac{(t - t_0 + (n-1)pP)}{W}\right]^2\right) \quad (1)$$

where, *t* is the time variable (bin) in a period
t_0 is the pulse position in a matched period
N is the total number of periods in the record, or *T* = *NP*.
n is the folded period number
P is the pulsar period
p is the period search factor
W is the pulsar pulse width
A(n) is the pulse amplitude in each period.

For modest signal-to-noise ratios this analysis provides measures useful for separating the pulsar pulse from large noise spikes or RFI by exploiting the characteristic amplitude, peak shift and shape around the search maximum.

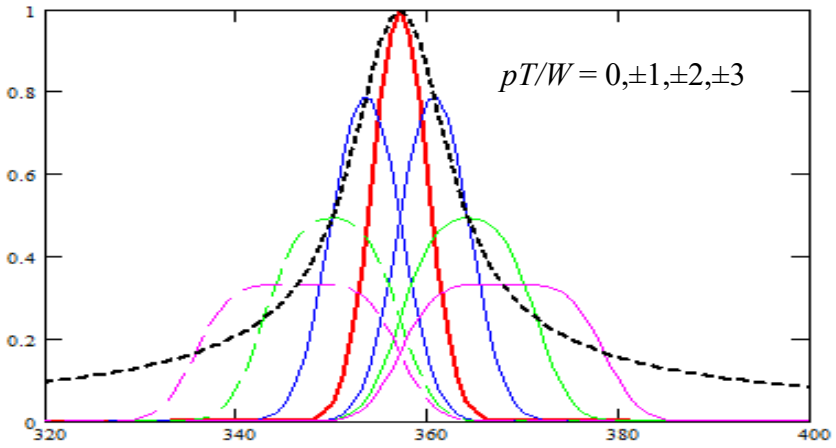

Figure 2. Pulse Shift, Amplitude Shape and Width Change for, $pT/W = 0,\pm1,\pm2,\pm3$

Figure 2 has been modeled assuming a Gaussian-shaped pulse; red, blue, green, magenta plot $pT/W = 0,-1,-2,-3$ (solid lines) and $pT/W = 0,+1,+2,+3$ (dotted lines) respectively. Figure 2 shows (black dotted line) the peak amplitude profile and pulse peak shift as a function of period variation for the parameter, pT/W.
For example, the half height amplitude profile width (green plots) occurs when,

$$p = \pm 2W/T$$

The locus of the maxima shown in Figure 2 (black dotted curve), is given by Equation (1) when $(t_0 - t) + (n-1)pP$ in the numerator is replaced by $(t_0 - t)(1-n/N)$. The half height width expected is, $\Delta p = 4W/T$; dependant on the pulsar pulse width and record time. The response will however be modified by scintillation, antenna pattern in drift scan and the folded noise features and these should all be taken into account.
Figure 3 is as observed for real data from a 2 hour record having a best candidate (red plot peaking at 357ms) signal-to-noise ratio of 4.5:1.

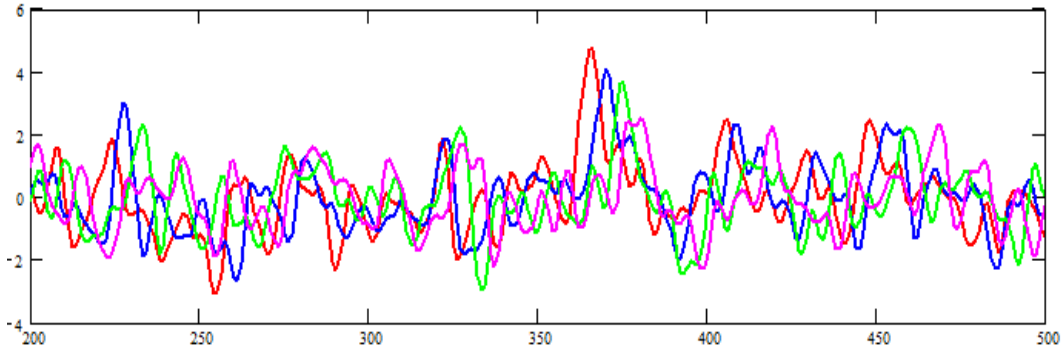

Figure 3. 4.5:1 SNR Data Result for, $pT/W = 0,-1,-2,-3$ (x-axis in ms)

Whilst Figure 3 shows the predicted amplitude variation and some indication of the broadening pulse width for the near-central candidate it is still affected by the underlying noise; however the effect on noise peaks is not so clear. Positive pT/W demonstrates similar effects but are not shown for clarity. A better presentation is to

sum equal magnitude positive and negative *pT/W* plots to accentuate the pulse broadening and average to some extent, the underlying noise.

Properties of Folding Noise

Noise peaks in the matched plot are the resultant summations of noise in period blocks along the record (see Figure 4). For true noise, they are not expected to result from a regular pattern but more likely random large summations anywhere along the record. An example is the (red) peak at 450ms in Figure 3; with decreasing period, this peak shifts but does not appear significantly attenuated. In fact, the shifts with changing *pT/W* are roughly equal in magnitude, implying that they arise from a single accumulated noise peak late in the data record. There is of course some corruption due to other period noise components, but it is evident that no other potential peaks show the predicted peak/amplitude/width variation as does the central candidate. Figure 4 shows another low SNR example with a six time-section waterfall representation. The amplitude resolution varies from red (highest), yellow, green, blue, and violet (lowest). The total sum plot is shown below.

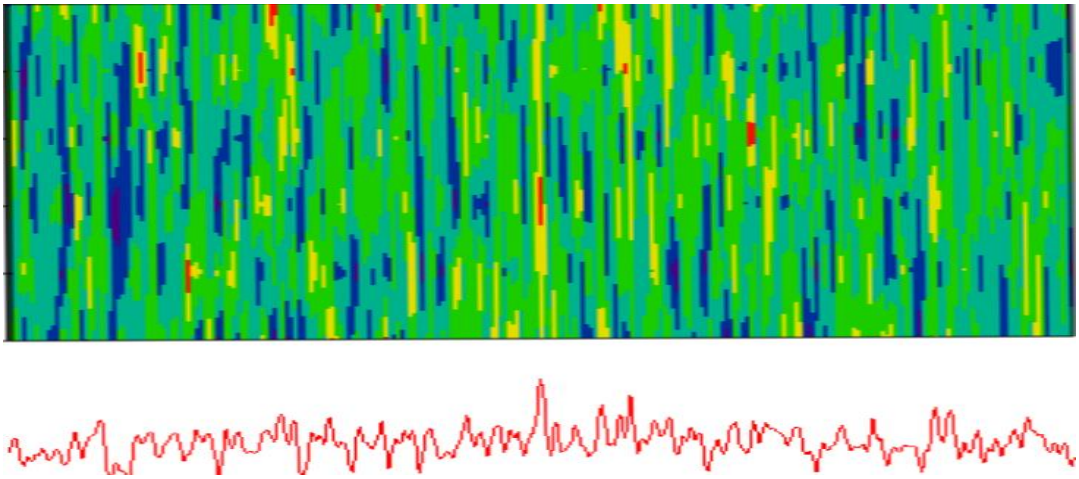

Figure 4. Waterfall Time Display Showing Noise Peaks and Continuous Pulsar Signal

It is noted that whereas the strongest central candidate is largely present (red, yellow) throughout the record duration, the bright noise peaks rarely correlate across consecutive time sections.

Pulsar p-dot (p^d), Search Characteristics

The p-dot search is designed to detect if there is any spin-down or apparent rotation rate change during the observation period. The fold period is gradually increased or decreased at a constant rate during the observation. The effects are somewhat similar to those of period search, but the apparent peak shift and shape are different.

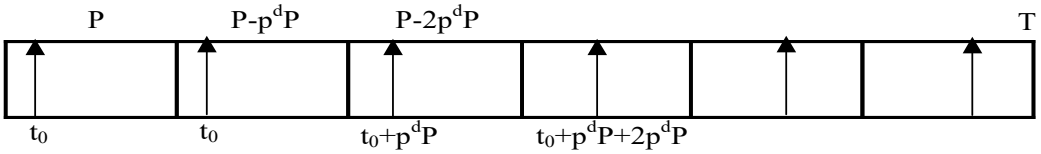

Figure 5. p-dot (p^d) Search parameters

As each period is progressively increased, the shifts sum and for large values of p-dot the spacing increases so pulses become separated and no longer add linearly.

The process in summary,

1. Again, when the fold period matches the pulsar period ($p^d = 0$) the pulsar pulses align in each fold period and add to maximize pulse visibility.
2. Decreasing the fold period rate slightly causes the pulse to increasingly shift later within the fold range smearing out the pulse.
3. The maximum shift occurs within the last fold period and totals, $\Sigma n p^d P$, where p^d is the fold period change, $p^d = \delta P/P$ and n is the period number.
4. If T is the total observation time, then the number of folds $N = T/P$ and the pulse total spread extent is $p^d T^2/2P$.
5. So, with p^d search period change per period, the mean pulse width increases to $p^d T^2/2P$ and the pulse median position changes to, $t_0 + p^d T^2/4P$. The apparent peak now lies nearer to zero in the region 0 to $p^d T^2/2P$.
6. Again, the pulse extent and shape and amplitude change are dependant on scintillation, but even for modest p-dot values the pulse energy is dissipated more rapidly that the straightforward search process.

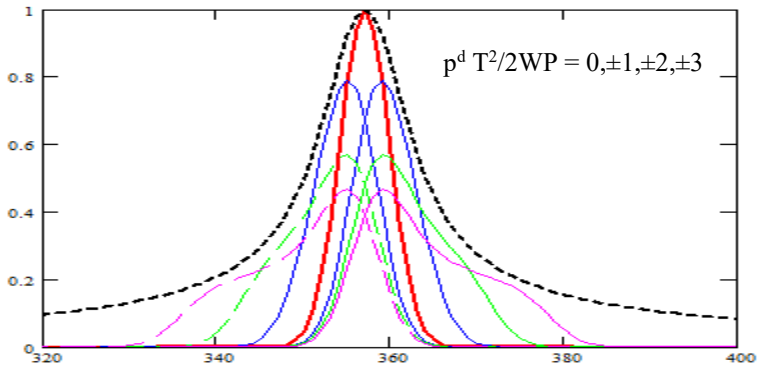

Figure 6. Pulse Shift, Amplitude Shape and Width Change for, $p^d T^2/2WP = 0,\pm1,\pm2,\pm3$

Figure 6 has been modeled assuming a Gaussian-shaped pulse; red, blue, green, magenta describe, $p^d\ T^2/2WP\ = 0,\pm1,\pm2,\pm3$ as before. Note all pulse extents lie within the previously calculated amplitude profile. These ideal plots have been derived using Equation (3) below after setting $p = 0$. Figure 7 shows the result observed for real data from a 2 hour record having a signal-to-noise ratio of 4.5:1.

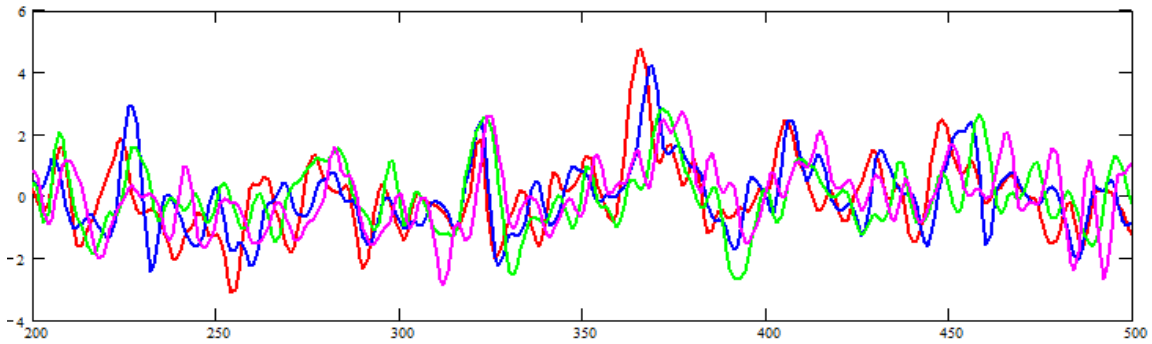

Figure 7. 4.5:1 SNR Data Result for, $p^d T^2/2WP = 0,-1,-2,-3$

Note that the peak amplitude and pulse widths of the best candidate follow the pattern in the previous slide, with some distortion due to the underlying noise no other data peak has the same characteristics showing that significant noise peaks are rarely consistent over the observation period.

Combined Period and p-dot Search Characteristics

Combining period and p-dot search allows the pulsar data along the data record to be explored.

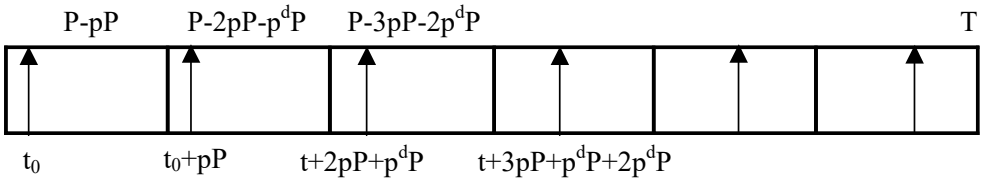

Figure 8. Combined Period and p-dot Search Parameters

The duration of the n^{th} block is $\{P - npP - (n\text{-}1)p^dP\}$ and the corresponding (maximum) pulse position shift is,

$$ps_{max} = +\{(N\text{-}1)pP + (N\text{-}1)(N\text{-}2)p^dP/2\} \qquad (2)$$

Equation (2) can be simplified by noting that $T = NP$, then $ps_{max} = pT + p^dT^2/2P$; where, T is the record duration.

Assuming the pulsar is similar to a Gaussian shaped pulse of width W, the fold algorithm can be expressed as,

$$Fold(t) = \frac{1}{N}\sum_{n=1}^{N} A(n) \exp\left(-4\ln(2)\left[\frac{\left(t - t_0 + (n-1)P\left(p + (n-2)p^d/2\right)\right)}{W} \right]^2 \right) \qquad (3)$$

where,

t is the time variable (bin) in a period

t_0 is the pulse position in a matched period

N is the total number of periods in the record

n is the folded period number

P is the pulsar period

p is the period search factor

p^d is the period rate of change factor

W is the pulsar pulse width

$A(n)$ is the pulse amplitude in each period.

For an equal distribution of pulses ($A(n)$ =1) along the data record, on folding, the resulting pulse will accumulate to produce a median, shifted by $ps_{max}/2$ and new pulse extent of ps_{max} when, $ps_{max} > W$ and approximately, W when, $ps_{max} < W$.

Equation (3) shows that choosing opposite polarities, the effects of period and p-dot search can be partially balanced out, extending the visibility of the pulsar pulse train. For example, by setting, $p^d = -2p/N$, the period search value ranges from $+p$ at the beginning of the record to $-p$ at the end. The resulting pulse suffers no delay shift but amplitude reduction and pulse width increase does occur with limits of half seen previously for a given variation, p. In this case, the period is matched at the record center. By suitably choosing p and p^d the matched period section can be tuned along the record to investigate various sub-sections of the data set.

Dispersion Measure Search

At a given radio frequency and RF band, it is convenient to describe the actual band dispersion, D observed in ms. For the RF band f_1 to f_2 chosen, D is calculated from,

$$D = 4.15\left(\frac{1}{f_1^2} - \frac{1}{f_2^2}\right) DM \ \ ms \qquad (4)$$

where, f_1 and f_2 are RF band edge frequencies in GHz and DM is the catalogued pulsar dispersion measure.

The effect of positive or negative dispersion away from D is to broaden the observed pulse width due to the lower frequencies natural delay. Modeling, using a Gaussian target pulse shape, the pulse broadening can be analyzed from the mean pulse response in a period,

$$P(t) = \frac{1}{Nf}\sum_{n=1}^{Nf} A(n)\exp\left(-4\ln(2)\left[\frac{\left(t - t_0 + \frac{n}{Nf}d - x\left(\frac{d}{2}\right)\right)}{W}\right]^2\right) \qquad (5)$$

where,

Nf is the number of RF sub-bands

n is the sub-band number

$A(n)$ is the average pulse amplitude in sub-band n

d is the test dispersion in ms in searching across the peak response.

The factor $x = 1$ if dispersion search is referenced to the band center (Figure 9b) or $x = 0$, if the dispersion is referenced to the band edge (Figure 9a).

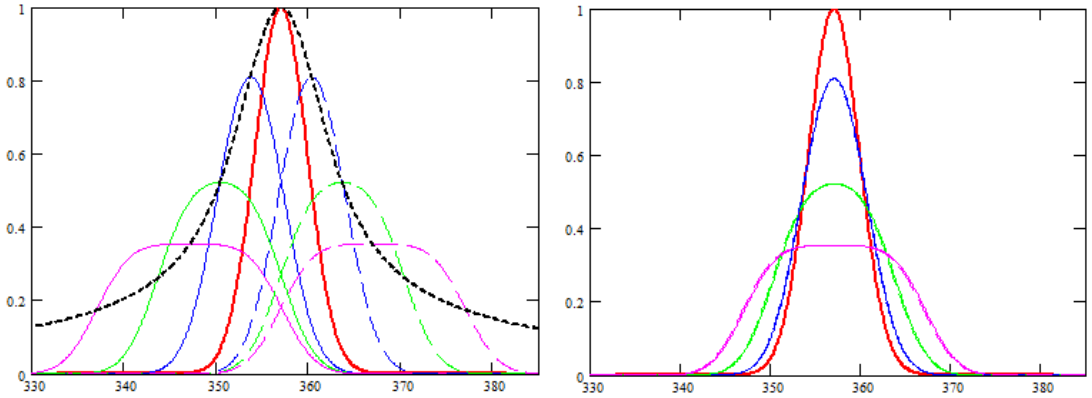

Figure 9. Dispersion Search Effects, d/W = 0, ±1, ±2, ±3

The locus of the maxima in Figure 9a (black dotted curve), is given by Equation (5) when $x = 0$ and d is replaced by, $(t_0 - t)$.

Figure 10 plots 4.5 SNR data. This clearly shows pulse broadening and amplitude reduction of the central candidate which is not shared by any other possible candidate peaks, confirming their random noise nature.

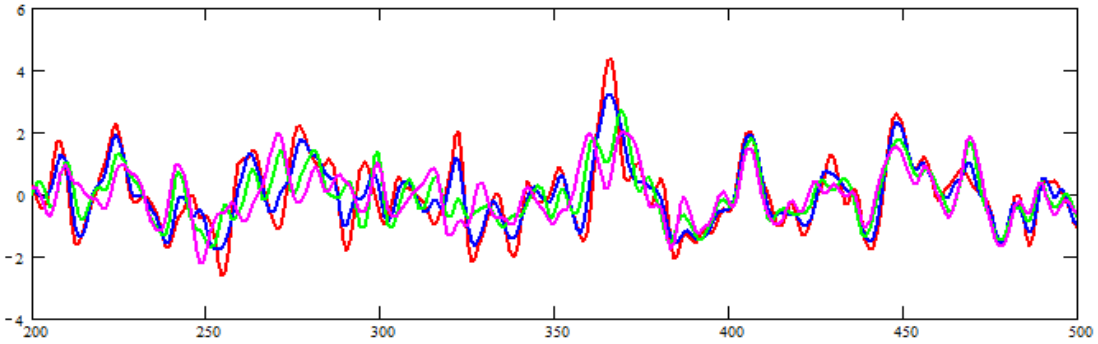

Figure 10. 4.5 SNR Dispersion Search, $d/W = 0,\pm1,\pm2,\pm3$, Band-centre Reference

Using PRESTO to Improve Low SNR Period and Dispersion Search Outcomes. Whilst the PRESTO period search, p-dot search and dispersion search plots give a good indication of pulsar parameters at large SNRs, they do not illustrate the peak offsets and profiles discussed above. However, the information is available for interpretation in associated best-profile files. By using an SNR plotter to graph the folded data when adjusting the command-line period/dispersion parameters, the analytic effects described in this paper can be observed. Note that in PRESTO with dispersion parameter (DM) change, the reference point is band edge referenced and the plots of Figure 9a are relevant. PRESTO also contains powerful algorithms for removing the effects of RFI so improving pulsar visibility - in one case increasing the observed SNR from 5:1 to 6:1.
Also, PRESTO pre-processed data followed by the analytical techniques described, further improves the chances of extracting low SNR pulsars

Conclusions

Detailed analysis of period search, p-dot search and dispersion search has shown that certain measurable features of pulsar properties are available for separating true pulsar signals from noise peaks. Specifically, pulsar peaks shift in a predictable manner as does the shape of the period-amplitude search curve. Tools have been derived allowing data responses to the various search routines to be predicted.
Scintillation adds a semi-random feature to the pulsar data that varies from day to day affecting search outcomes. For example, period and p-dot search properties derived are affected by scintillation whereas dispersion search is not, making this a much stronger pulsar indicator.
Whilst the examples given relate to real data with an SNR around 4.5:1, accumulation of the features analyzed significantly improves the feasibility of pulsar recognition to lower SNRs.

References

1. Keith MJ et al, 'Discovery of 28 pulsars using new techniques for sorting pulsar candidates' Mon.Not. R. Astron.Soc. 395, pp837-846(2009)
2. http://www.rfcafe.com/references/electrical/ew-radar-handbook/receiver-sensitivity-noise.htm
3.http://pws.npru.ac.th/sartthong/data/files/Radar%20Systems%20Analysis%20and%20Design%20Using%20MatLab%20-%20Mahafza%20Bassem%20R.pdf. Chapter 4.
4. https://download.collobos.com/en/Presto/files/UserGuide.pdf
5. East PW. A Minimal Pulsar Detection System. Journal of the Society of Amateur Radio Astronomers. January-February 2018. p36.